

Hsp70 and Hsp40 attenuate formation of spherical and annular polyglutamine oligomers by partitioning monomer

Jennifer L Wacker¹, M Hadi Zareie², Hanson Fong², Mehmet Sarikaya² & Paul J Muchowski¹

Protein conformational changes that result in misfolding, aggregation and amyloid fibril formation are a common feature of many neurodegenerative disorders. Studies with β -amyloid (A β), α -synuclein and other amyloid-forming proteins indicate that the assembly of misfolded protein conformers into fibrils is a complex process that may involve the population of metastable spherical and/or annular oligomeric assemblies. Here, we show by atomic force microscopy that a mutant huntingtin fragment with an expanded polyglutamine repeat forms spherical and annular oligomeric structures reminiscent of those formed by A β and α -synuclein. Notably, the molecular chaperones Hsp70 and Hsp40, which are protective in animal models of neurodegeneration, modulate polyglutamine aggregation reactions by partitioning monomeric conformations and disfavoring the accretion of spherical and annular oligomers.

A prominent feature of many neurodegenerative disorders is the accumulation of insoluble, aggregated protein inside and outside of neurons. The neuropathological lesions associated with each disease contain fibrillar deposits of distinct proteins, such as A β in Alzheimer disease, α -synuclein in Parkinson disease and the huntingtin protein in Huntington disease. Notably, the structural and biochemical characteristics of the fibrils formed in each pathological condition, including high β -sheet content and detergent insolubility, are conserved among disease-associated proteins despite having unrelated primary amino acid sequences and quaternary native structures¹. Recent structural and biochemical analyses of A β and α -synuclein have shown that aggregation is a complex, potentially multistep process involving the population of transient or metastable intermediates that are observed before or accompanying fibril accumulation². Size-exclusion chromatography and atomic force microscopy (AFM) were used to identify globular oligomeric assemblies termed ADDLs (A β -derived diffusible ligands) and short rod-shaped protofibrils composed of A β peptides that were proposed to be on-pathway intermediates for fibril formation^{3–5}. Similarly, AFM analysis showed that α -synuclein assembles into several structural species including spherical oligomers, protofibrils and pore-like annular structures that may be precursors to fibril formation^{6–9}. Huntington disease is a neurodegenerative disorder caused by an expansion of CAG repeats (encoding polyglutamine (polyQ)) in the gene *IT-15*, which encodes the huntingtin protein¹⁰. Although the polyQ repeat is polymorphic in the normal population, expansion above a critical threshold (~35–40) invariably results in disease. Biochemical studies with huntingtin fragments demonstrated that

polyQ tracts in the disease-causing range (>39) form detergent-insoluble protein aggregates that exhibit many properties characteristic of amyloid fibrils, whereas fragments with nonpathogenic repeat lengths do not aggregate¹¹. Although these studies focused on the end stage of polyQ aggregation reactions (fibril formation), it remains uncharacterized whether polyQ proteins form spherical and annular oligomeric structures similar to those reported for A β and α -synuclein.

All cells and organelles have a machinery of molecular chaperones whose function is to mediate the proper folding of other proteins and to ensure that these proteins maintain their native conformations during conditions of stress¹². Hsp70 and Hsp40 are two major cytosolic chaperones that suppress neurodegeneration in animal models of Huntington disease and Parkinson disease¹³. Hsp70 and Hsp40 act in a cooperative, ATP-dependent manner to bind and release unfolded and misfolded substrates, thereby enhancing substrate refolding and preventing inappropriate protein interactions that lead to aggregation. Although the mechanism of Hsp70 and Hsp40 in protein folding has been characterized extensively with model substrates, little is known about how these chaperones may influence the assembly of misfolded protein conformers into amyloid fibrils. In one study, Hsp70 and Hsp40 suppressed partially the accumulation of SDS-insoluble aggregates formed by a mutant huntingtin fragment, as measured by a filter retardation assay¹⁴. Notably, the chaperones were effective only when added during the lag phase of the aggregation reactions, suggesting that Hsp70 and Hsp40 act on early, structurally undefined intermediates in the polyQ assembly process.

The purpose of this study was to characterize structurally different assemblies formed by a mutant huntingtin fragment during aggregation

¹Department of Pharmacology and ²Department of Materials Science and Engineering, University of Washington, Seattle, Washington, 98195-2120, USA. Correspondence should be addressed to P.J.M. (muchowski@u.washington.edu).

Published online 14 November 2004; doi:10.1038/nsmb860

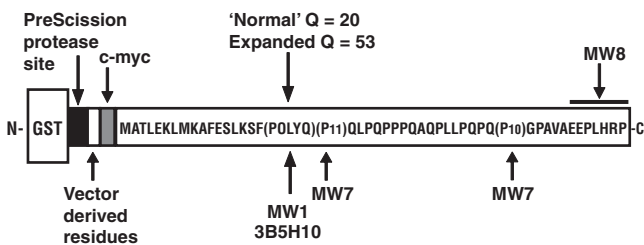


Figure 1 Experimental system used to study the aggregation of a mutant huntingtin fragment. A schematic representation of the GST-huntingtin exon 1 fusion protein (HD20Q or HD53Q) shows a PreScission protease site located between GST and the huntingtin fragment (not drawn to scale), and the locations of antibody epitopes (c-myc, MW1, MW7, MW8 and 3B5H10) that were used as probes in biochemical assays.

reactions and to determine how Hsp70 and Hsp40 may modulate such assemblies. Here we present two major findings. First, we demonstrate that a mutant huntingtin fragment with an expanded polyQ repeat forms spherical and annular oligomeric assemblies that are similar in size and morphology to those formed by A β and α -synuclein. Second, we show that Hsp70 and Hsp40 act cooperatively in an ATP-dependent manner to partition monomeric conformations of the mutant huntingtin fragment, and concomitantly attenuate formation of spherical and annular polyQ oligomers.

RESULTS

Detection of spherical and annular polyQ oligomers

Proteins encoding the first exon of huntingtin with polyQ repeats in the normal (HD20Q) and pathogenic (HD53Q) range (Fig. 1) were purified from *Escherichia coli* as fusions to glutathione S-transferase (GST)¹⁴. After purification, GST-HD20Q and GST-HD53Q were detergent-soluble and appeared nonaggregated by AFM analysis (data not shown). Incubation of the fusion proteins with a site-specific protease resulted in the removal of the GST moiety and release of the huntingtin fragments. After proteolytic cleavage, HD53Q immediately begins to aggregate and assembles into fibrils in a concentration- and time-dependent manner¹⁵. In contrast, HD20Q remains soluble after GST cleavage and does not assemble into fibrils (data not shown).

We first used AFM to characterize structures formed by HD53Q at 6 and 20 μ M, concentrations determined empirically to be below the critical concentration required for fibril formation, over a 5-h time course (Fig. 2). At 6 and 20 μ M HD53Q, the dominant structure observed in 3 μ m² scans 1 h after GST cleavage was a heterogeneous population of spherical assemblies with a diameter of 5–65 nm (Fig. 2d,f arrows). At 5 h after GST cleavage in the 6 μ M HD53Q reaction, the average diameter (60–125 nm) of these spherical structures had increased and their morphology became amorphous (Fig. 2b, arrows). At 5 h after GST cleavage in the 20 μ M HD53Q reaction, a high-density (defined herein as particles/field) of annular structures (average diameter, 105 nm), similar

Figure 2 A mutant huntingtin fragment forms spherical, annular and fibrillar structures in a concentration- and time-dependent manner. (a–f) Representative 3 μ m² AFM images of 6, 20 and 60 μ M HD53Q aggregation reactions at 1 h (a, c, e) and 5 h (b, d, f) after cleavage of the GST moiety from HD53Q. Spherical structures were observed at 1 h at all concentrations (arrows, a, c, e). At 5 h, many amorphous aggregates were apparent in the 6 μ M reaction (arrows, b), whereas numerous annular structures were observed in the 20 μ M reaction (arrows, d). In the 60 μ M reaction, fibrils were detected at 1 h and increased in density by 5 h (e, f). Scale bar, 500 nm.

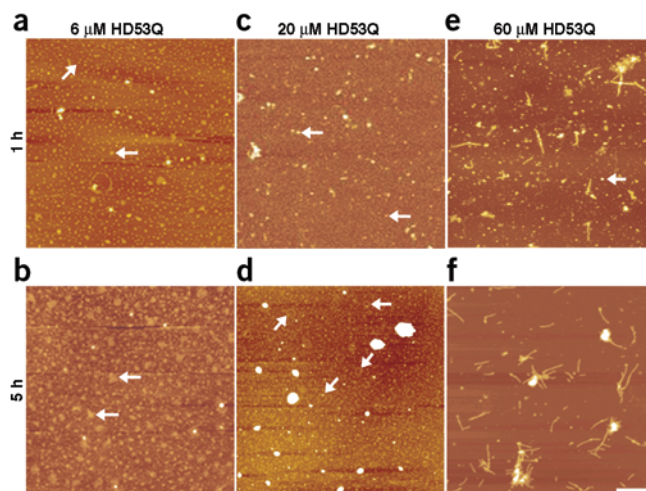
in morphology and size to those reported previously for α -synuclein⁹, were detected (Fig. 2d, arrows). Analysis of the topography of an annular structure showed that it was composed of a discontinuous ring of smaller, short and elongated annular structures (see Supplementary Fig. 1 online).

AFM analysis of a 60 μ M HD53Q reaction at 1 h after GST cleavage showed an accumulation of fibrils that coexisted with small spherical assemblies (5–75 nm in diameter) and some amorphous aggregates (Fig. 2e). Fibrils varied from 90 to 440 nm in length and had an average width of 20 nm. Between 1 and 5 h there was, on average, a 3.3-fold increase ($P < 0.05$) in fibril density concomitant with a statistically significant decrease ($P < 0.05$) in the density of spherical assemblies (Figs. 2f and 3).

Hsp70 and Hsp40 attenuate formation of polyQ oligomers

We next used AFM to characterize the effects of Hsp70 and Hsp40 on HD53Q assembly into spherical and annular oligomeric structures. Purified Hsp70 and Hsp40 were added to the aggregation reactions at time zero, along with protease. Co-incubation of 6 μ M HD53Q with an equimolar concentration of Hsp70 and Hsp40, in the presence of ATP and an ATP-regenerating system, resulted in a statistically significant reduction in the density of spherical assemblies concomitant with an increase fibril density between 1 and 5 h (Figs. 3 and 4). A more pronounced result was observed with 20 μ M HD53Q in the presence of Hsp70 and Hsp40 (Fig. 4e, f and 3). On average, the chaperones caused a 3.6-fold ($P < 0.05$) and 2.2-fold ($P < 0.05$) increase in fibril density in the 6 and 20 μ M HD53Q reactions between 1 and 5 h, respectively, which paralleled a statistically significant decrease ($P < 0.01$ and $P < 0.05$, respectively) in the density of spherical oligomers (Fig. 3). Notably, fibrils were never observed in the 6 and 20 μ M HD53Q aggregation reactions in the absence of Hsp70 and Hsp40, but were easily detected at 1 h in the presence of chaperones (Fig. 4a, e). The fibrils that accumulated in the presence of chaperones ranged from 80 to 475 nm in length and 12 to 18 nm in width, similar in magnitude to the fibrils formed in the absence of chaperones. Large, amorphous structures were also observed in the presence of chaperones and HD53Q, as described previously using transmission EM (TEM)¹⁴, although AFM analysis showed that fibrillar HD53Q structures were clearly an abundant species 5 h after GST cleavage (Fig. 4e, f). Our results indicate that HD53Q forms spherical and annular oligomeric structures at low concentrations, and that these structures disappear at high concentrations, or at low concentrations in the presence of Hsp70 and Hsp40.

Do spherical oligomeric structures formed by HD53Q fuse to form fibrils, and do chaperones directly partition spherical oligomers into



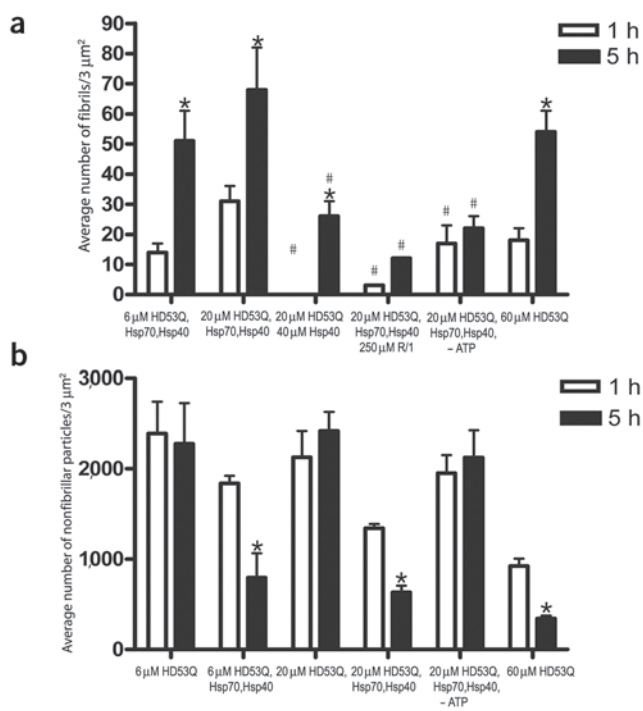


Figure 3 Quantitative analysis of particle density in 3 μm² AFM scans. **(a)** Fibril density from three independent AFM scans was calculated for the 6 μM and 20 μM HD53Q reactions in the absence and presence of Hsp70 and Hsp40 and R/1, a specific inhibitor of the ATPase activity of Hsp70 (ref. 16), and for the 60 μM HD53Q reaction in the absence of Hsp70 and Hsp40. The averages and s.d. for the 1 and 5 h time points are graphed. Note that fibrils were not detected in the 6 μM and 20 μM HD53Q reactions in the absence of Hsp70 and Hsp40. Asterisk denotes a significant difference in fibril density ($P < 0.05$) between 1 and 5 h. Number sign (#) denotes a significant difference in fibril density between reactions in the presence of chaperones. **(b)** The density of nonfibrillar structures (spherical, annular and amorphous) from three independent AFM scans was calculated for the 6 μM and 20 μM HD53Q reactions in the presence and absence of Hsp70 and Hsp40, for the 20 μM HD53Q reaction in the presence of Hsp70 and Hsp40 but in the absence of ATP, and for the 60 μM HD53Q reaction in the absence of Hsp70 and Hsp40.

each chaperone alone did not cause a marked decrease in the accumulation of polyQ oligomers at 1 or 5 h (see **Supplementary Fig. 2** online). At 5 h in the presence of excess Hsp40, several short fibrils were observed, suggesting that the activity of Hsp40 alone may be sufficient to promote modest fibril accumulation. However, the density of fibrils was significantly lower ($P < 0.05$) than that observed in the presence of Hsp70, Hsp40 and ATP (**Fig. 3**). These results indicate that Hsp70 and Hsp40 cooperate to decrease the accumulation of spherical and annular HD53Q assemblies, and that the accumulation of fibrils observed in the presence of chaperones is independent of macromolecular crowding effects.

To confirm that the chaperone-mediated decrease in accumulation of spherical and annular oligomeric structures was dependent on the ATPase activity of Hsp70, two experiments were conducted. First, we used AFM to analyze the 20 μM HD53Q aggregation reactions incubated with equimolar Hsp70 and Hsp40 (added at time zero) in the absence of ATP (**Fig. 5a,b**). Under these conditions, fibril formation was largely suppressed at 1 h and the majority of protein appeared in spherical assemblies. By 5 h there was a small increase in fibril accumulation,

fibrils? To address these questions, the following order of addition experiments were conducted. AFM analysis was carried out on 6 and 20 μM HD53Q aggregation reactions in which equimolar Hsp70 and Hsp40 were added at 1 h after GST cleavage, a time point at which spherical assemblies predominate in the absence of chaperones. Under these conditions, fibril accumulation was not apparent at 1 h (**Fig. 4c,g**) or 5 h (**Fig. 4d,h**) after chaperone addition. Rather, a heterogeneous population of spherical oligomeric assemblies and amorphous aggregates persisted, similar to those that formed in the absence of chaperones (compare **Figs. 4c,d** and **2a,b**, as well as **Figs. 4g,h** and **2c,d**). These results indicate that Hsp70 and Hsp40 act on a conformation of HD53Q that precedes or is independent of the formation of spherical structures, and cannot disassemble preformed spherical structures. These results, however, do not exclude the possibility that spherical structures could serve as nuclei or seeds onto which monomers are added to result in fibril growth. To address the latter possibility, AFM analysis was carried out on 6 μM HD53Q aggregation reactions in which equimolar Hsp70 and Hsp40 were added at 1 h after GST cleavage concomitant with a fresh aliquot of nonaggregated 6 μM HD53Q to serve as a pool of monomers. Under these experimental conditions, robust fibril accumulation was not observed (data not shown), suggesting that spherical oligomers may be off-pathway for polyQ fibril formation. We next tested whether Hsp70 and Hsp40 cooperate to decrease the accumulation of spherical and annular HD53Q assemblies. AFM analysis was carried out on 20 μM HD53Q aggregation reactions with 40 μM Hsp70 or Hsp40 alone added at time zero. Under these conditions,

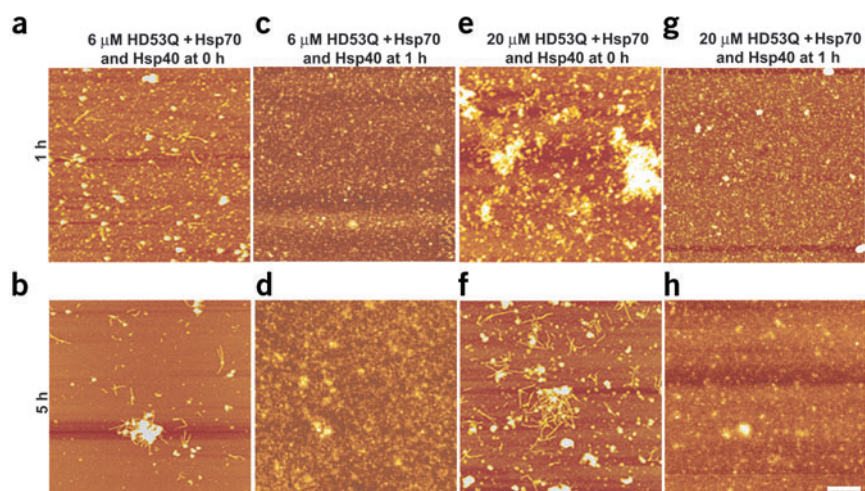


Figure 4 Hsp70 and Hsp40 chaperones attenuate formation of spherical and annular oligomeric structures by a mutant huntingtin fragment. **(a–h)** Representative 3 μm² AFM images of 6 μM **(a,b)** and 20 μM **(e,f)** HD53Q reactions in which equimolar Hsp70 and Hsp40 and ATP were added at time zero indicate an attenuation of the formation of spherical and annular structures and an increase in accumulation of fibrils between 1 and 5 h. Addition of equimolar Hsp70 and Hsp40 to the 6 μM **(c,d)** and 20 μM **(g,h)** HD53Q reactions at 1 h after GST cleavage (when spherical structures predominate) did not attenuate formation of spherical and annular structures, and did not show an increased accumulation of fibrils when measured at 1 and 5 h after chaperone addition. Scale bar, 500 nm.

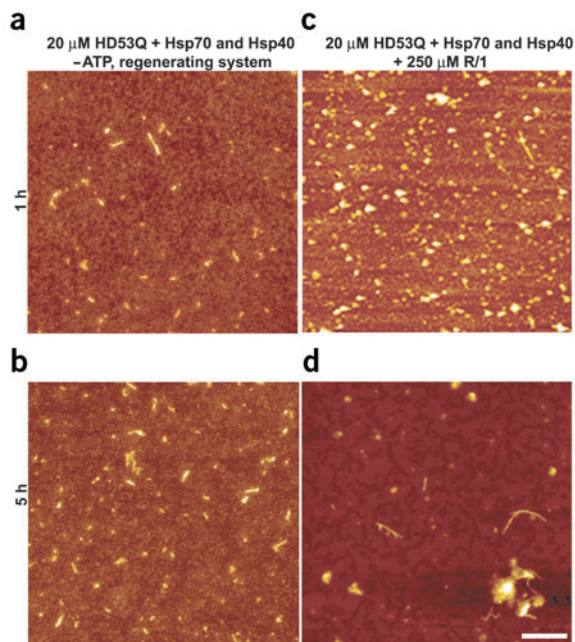


Figure 5 ATP and Hsp70 ATPase activity are necessary for the attenuation of spherical and annular structures formed by a mutant huntingtin fragment. (a,b) Representative $3 \mu\text{m}^2$ AFM scans of a $20 \mu\text{M}$ HD53Q aggregation reaction with equimolar Hsp70 and Hsp40 at 1 h (a) and 5 h (b) after GST cleavage in the absence of ATP. (c,d) Representative $3 \mu\text{m}^2$ AFM scans of a $20 \mu\text{M}$ HD53Q aggregation reaction with equimolar Hsp70 and Hsp40 at 1 h (c) and 5 h (d) after GST cleavage in the presence of R/1, a specific inhibitor of the ATPase activity of Hsp70 (ref. 16). Scale bar, 500 nm.

antibodies over the 5 h time course, and showed only a slight increase in the MW7 and MW8 signal after GST cleavage (Fig. 6a–d). The nonpathogenic HD20Q protein reacted equally well with the MW8 (Fig. 6e) and MW7 (see Supplementary Fig. 3 online) antibodies over the 5 h time course, demonstrating that the occlusion observed in the HD53Q reactions is specific for the expanded polyQ repeat. As expected, the MW1 and 3B5H10 antibodies, which selectively recognize a structural epitope found only in expanded polyQ repeats, did not react with the HD20Q fusion protein (data not shown). Collectively, these results indicate that under nondenaturing conditions antibodies that recognize the expanded polyQ region in HD53Q preferentially detect nonaggregated protein and fibrils, but not spherical and annular oligomeric species.

Hsp70 and Hsp40 suppress polyQ epitope occlusion

Our AFM results showed that in the 6 and $20 \mu\text{M}$ HD53Q reactions, Hsp70 and Hsp40 decreased the accumulation of spherical and annular oligomeric structures. Furthermore, slot-blot analyses showed that once formed, these nonfibrillar species exhibit a marked decrease in reactivity to antibodies that recognize the polyQ repeat in HD53Q. If chaperones attenuate formation of spherical and annular oligomeric structures, one would predict that the loss of polyQ epitope accessibility observed in these structures by slot-blot assays could be rescued by addition of chaperones to the aggregation reactions at time zero. Indeed, addition of equimolar Hsp70 and Hsp40 to the $6 \mu\text{M}$ HD53Q reactions caused a robust increase in HD53Q epitope accessibility to the MW1, 3B5H10 and MW8 antibodies at 1 and 5 h (Fig. 6a–d), whereas reactivity to HD20Q, which remains soluble over the time course, did not increase in the presence of chaperones (Fig. 6e and see Supplementary Fig. 3 online). The $20 \mu\text{M}$ HD53Q reactions showed a similar, but less robust increase in antibody binding in the presence of Hsp70 and Hsp40. As with the AFM results, an increase in epitope accessibility required the cooperative activity of Hsp70, Hsp40 and ATP, and chaperones were effective only when added at time zero (data not shown).

Hsp70 and Hsp40 partition SDS-soluble polyQ monomers

We and others have previously shown that Hsp70 and Hsp40 partially increase the detergent solubility of aggregating polyQ species *in vitro* and *in vivo*^{14,18}. Because on the surface these previous results seemed to contradict our AFM results, which showed that Hsp70 and Hsp40 decrease accumulation of spherical and annular oligomeric structures while some fibrils are still formed, we next determined whether HD53Q assemblies generated in the presence of chaperones showed altered biochemical properties. Sedimentation analysis, used previously to analyze the proportion of aggregating α -synuclein species that can be pelleted by high-speed centrifugation¹⁹, was used to monitor HD53Q aggregation in the absence and presence of Hsp70 and Hsp40. At time zero, 6 and $20 \mu\text{M}$ HD53Q were detected only in the supernatant fraction and migrated in SDS gels as monomeric species (Fig. 6f). In these reactions HD53Q was absent entirely from the supernatant and redistributed to the pellet fraction 1 h after GST cleavage, running as SDS-insoluble species at the interface between the stacking and resolving gel (Fig. 6f). These results

although the density of fibrils was significantly lower ($P < 0.05$) than that observed in the presence of Hsp70, Hsp40 and ATP (Fig. 3). Moreover, most fibrils were < 100 nm in length, significantly shorter than those generated in the presence of Hsp70, Hsp40 and ATP. We next tested the effects of a small molecule inhibitor (NSC630668-R/1, referred to as R/1) of the endogenous and Hsp40-stimulated ATPase activity of Hsp70 (ref. 16). AFM analysis of $20 \mu\text{M}$ HD53Q with Hsp70, Hsp40, ATP and R/1 showed a preponderance of spherical oligomers and a strong reduction in fibril accumulation at 1 and 5 h after GST cleavage (Fig. 5c,d).

The polyQ repeat is buried in oligomeric structures

We next used a slot-blot assay to monitor the reactivity of aggregating HD53Q species to a panel of antibodies in the absence and presence of chaperones (antibody epitopes on HD53Q, Fig. 1). A similar slot-blot assay was used previously to show that A β , α -synuclein and polyQ peptides adopt a structural epitope found only in soluble oligomeric structures that correlates with cellular toxicity¹⁷. This assay was used to detect changes in antibody epitope accessibility at selected time points and concentrations of HD53Q. Under all experimental conditions, an equal amount of total protein was removed from aggregation reactions and diluted in a nondenaturing buffer (lacking SDS) before being applied to the nitrocellulose membrane (Fig. 6). At $6 \mu\text{M}$ HD53Q, a concentration in which spherical assemblies predominate (Fig. 2a), slot-blot analysis showed that the epitopes for two distinct monoclonal antibodies (3B5H10 and MW1) that recognize the polyQ repeat in HD53Q were progressively masked between 0 and 5 h (Fig. 6b,d). A similar, though less robust epitope occlusion was also evident in the $20 \mu\text{M}$ HD53Q aggregation reactions when probed with the 3B5H10 and MW1 antibodies (Fig. 6b,d). In contrast, antibodies whose epitopes map outside of the polyQ repeat (MW8, MW7 (Fig. 6a,c) and c-myc (data not shown)) showed modest or no antibody occlusion in the $6 \mu\text{M}$ reactions and no occlusion in the $20 \mu\text{M}$ reactions, suggesting that these epitopes are solvent-exposed on the outside surface of spherical and annular oligomeric structures. Notably, despite loading of an equal amount of protein on the membrane, the $60 \mu\text{M}$ HD53Q reactions, which are composed predominantly of fibrils as determined by AFM (Fig. 2e,f), reacted equally well with the 3B5H10 and MW1

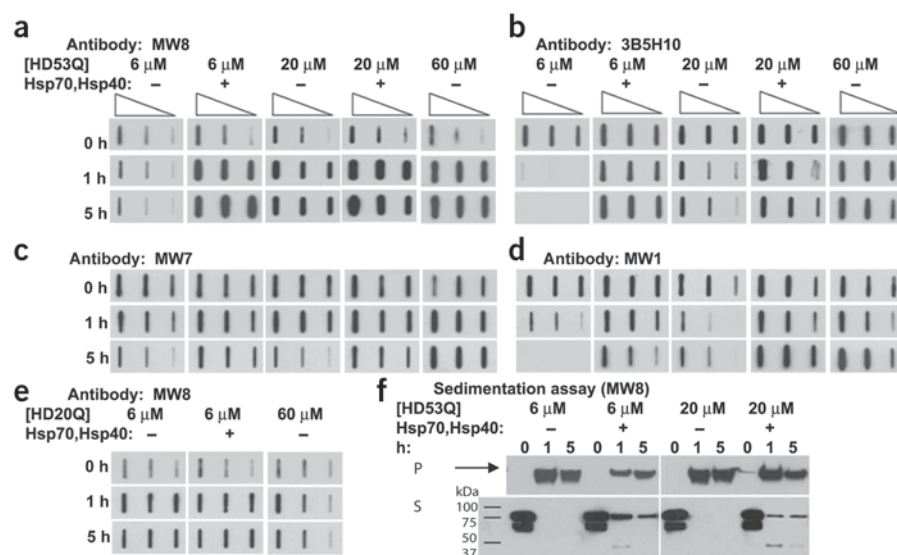


Figure 6 Hsp70 and Hsp40 expose polyQ epitopes that are normally buried in spherical and annular oligomeric structures formed by a mutant huntingtin fragment. Slot blot analyses of HD53Q and HD20Q reactions in the absence or presence of Hsp70 and Hsp40. (**a–e**) Aliquots containing equal amounts of HD53Q (or HD20Q) protein in the absence and presence of Hsp70 and Hsp40 were removed from aggregation reactions before cleavage (0 h), at 1 and 5 h after GST cleavage, and were spotted under nonreducing conditions onto a nitrocellulose membrane as a dilution series of 1 μg, 0.5 μg and 0.25 μg protein. The membranes were next probed with selected monoclonal antibodies (MW8, 3B5H10, MW7 and MW1; see Fig. 1 for epitopes). Antibodies directed at the polyQ tract (MW1 and 3B5H10) were occluded as spherical and annular structures accumulated, whereas addition of Hsp70 and Hsp40 in HD53Q aggregation reactions maintained these epitopes available for antibody binding throughout the time course of aggregation. (**e**) Reactivity of HD20Q with the MW8 antibody does not change with time or concentration, in the absence or presence of the chaperones. (**f**) Hsp70 and Hsp40 maintain a significant fraction of protein in an SDS-soluble, monomeric state during HD53Q aggregation reactions. Shown are representative results from sedimentation analyses of HD53Q aggregation reactions in the absence and presence of Hsp70 and Hsp40. After GST cleavage, high-molecular-mass, SDS-resistant complexes form in the pellet (P) that remain in the stacking gel (arrow). In the presence of Hsp70 and Hsp40, the amount of these SDS-resistant structures decreases significantly, whereas the amount of SDS-soluble, monomeric HD53Q in the supernatant (S) increases.

able to assemble into SDS-insoluble aggregates that correspond presumably to fibrils and not oligomeric structures.

DISCUSSION

An accumulation of evidence has led to the hypothesis that spherical and annular oligomeric structures may mediate neuronal dysfunction and cell death in neurodegenerative diseases associated with protein misfolding, and that the fibrillar forms of misfolded proteins may be inert or even neuroprotective². The first major finding reported in this study is a demonstration by AFM that a mutant huntingtin fragment with an expanded polyQ repeat (HD53Q) assembles into spherical and annular structures, similar in size and morphology to those formed by Aβ and α-synuclein, when analyzed at low concentrations that preclude fibril formation. Putative prefibrillar polyQ structures have been reported using TEM^{20,21}, and resemble the spherical oligomers that we observe with HD53Q by AFM. We propose the following model to describe the assembly of polyQ-containing proteins into fibrils (Fig. 7a). This model posits that multiple misfolded conformations of polyQ monomer coexist that can give rise to several distinct off-pathway assemblies (spherical, annular and/or amorphous structures), or alternatively can be incorporated directly into a growing fibril by monomer addition to structurally undefined fibril nuclei. In this model only one altered conformation of misfolded polyQ monomer can be directly incorporated into a growing fibril, and thus metastable off-pathway spherical, annular and amorphous structures compete with and decrease the likelihood of

spherical and annular structures formed by HD53Q as determined in AFM analyses under identical conditions are predominantly SDS-resistant. An equimolar concentration of Hsp70 and Hsp40 in the 6 μM HD53Q reaction reduced substantially the amount of pelleted or aggregated HD53Q in the stacking gel (Fig. 6f). Quantification of three experiments showed an average decrease of 47% (±5.8) at 1 h and 29% (±5.1) at 5 h. The remaining ~71% of aggregates that could not be solubilized by SDS under these conditions correspond presumably to the fibrils that were observed by AFM under identical conditions (Fig. 4). Consistent with these findings, chaperones caused a significant increase in a SDS-soluble monomeric HD53Q species present in the supernatant fraction (Fig. 6f), on average, 31% (±2.3) at 1 h and 19% (±1.8) at 5 h. Similar to the results of the slot-blot assay, a more moderate effect of Hsp70 and Hsp40 was observed in the 20 μM HD53Q reactions in the sedimentation assay. Addition of equimolar Hsp70 and Hsp40 to the 20 μM reaction reduced the amount of protein in the stacking gel 12.1% (±5.6) at 1 h and 40.3% (±5.5) at 5 h. The supernatant fraction showed that equimolar Hsp70 and Hsp40 maintained a substantial portion of HD53Q SDS-soluble at 1 and 5 h, 25.4% (±7.6) and 12.1% (±4.7), respectively. These results collectively indicate that when incubated with an equimolar concentration of HD53Q, Hsp70 and Hsp40 partition a substantial fraction of HD53Q into a SDS-soluble, monomeric state (~10–20%), whereas the majority of HD53Q (~60–70%) is still

on-pathway conformations that result in monomer addition to fibril nuclei (Fig. 7a). The rate-limiting step in this model is the formation of the proper misfolded monomeric polyQ conformation that gives rise to fibril formation, consistent with recent kinetic studies on the aggregation of polyQ peptides, which suggest that the aggregation nucleus is a monomer²². Notably, the structural transition that leads to fibril formation is favored only at high protein concentrations, well above that required to form spherical structures that do not appear to act as fibril nuclei. However, our experiments do not allow us to formally exclude an alternate model in which a misfolded conformation of a polyQ monomer self-associates to generate a spherical structure that then serves as an obligate intermediate or nucleation site for any one of several possible higher-order assemblies, including annular structures, amorphous structures or fibrils (Fig. 7b). In this alternate model only the spherical structures are on-pathway intermediates for fibril formation, and therefore annular and amorphous structures are metastable off-pathway assemblies that compete with and decrease the likelihood of on-pathway interactions that promote fibril formation (Fig. 7b). The rate-limiting step in this model would be the formation of a spherical intermediate that acts as a seed for higher-order assemblies. Although the data in this study does not support this model, a recent study with Sup35, a yeast prion that assembles into amyloid fibrils, showed that a spherical oligomer is an obligate intermediate for nucleating fibril

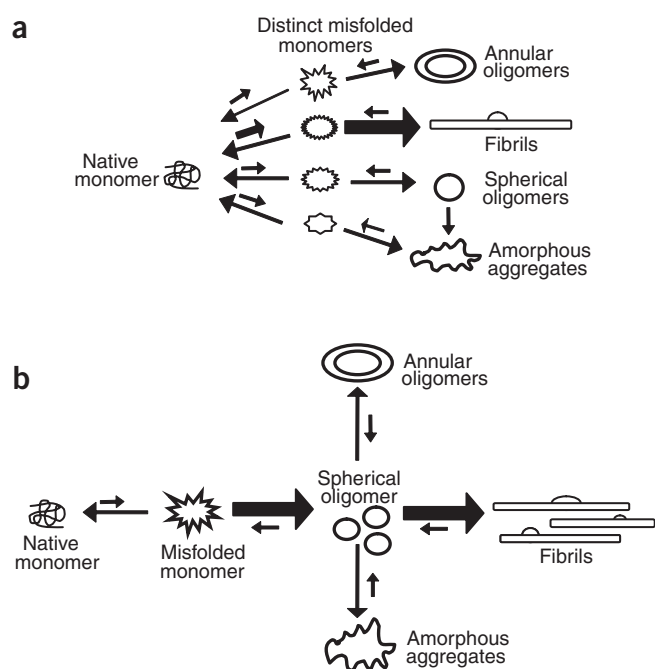


Figure 7 Two models for the assembly of expanded polyQ proteins into amyloid-like fibrils. **(a)** In the first model, monomers may exist in a number of distinct misfolded conformations. Only one altered conformer is on-pathway for fibril formation (bold arrows), and thus spherical, annular and amorphous structures are metastable off-pathway assemblies that compete with and decrease the likelihood of on-pathway interactions that promote fibril formation. In this model Hsp70 and Hsp40 facilitate the folding of a misfolded monomeric conformation of HD53Q to the native state or to a conformation that allows on-pathway assembly to occur by monomer addition to fibril nuclei. **(b)** In the second model, spherical oligomeric structures are obligate on-pathway intermediates for fibril assembly (bold arrows), whereas annular and amorphous structures are metastable off-pathway assemblies that compete with and decrease the likelihood of on-pathway interactions that promote fibril formation. In this model, Hsp70 and Hsp40 enhance fibril accumulation because of a rapid accumulation of spherical prefibrillar intermediates that are immediately converted to fibrils. According to this model, fibrillar structures represent a lower energy state than metastable off-pathway assemblies, thus accounting for the rapid appearance of fibrils. The data presented in this manuscript are most consistent with the former model, although the latter model has been proposed for Sup35, a yeast prion that assembles into amyloid fibrils²³.

formation *de novo*²³. The second major finding is that the molecular chaperones Hsp70 and Hsp40 act cooperatively in an ATP-dependent fashion to attenuate formation of spherical and annular assemblies by partitioning monomeric conformations of a mutant huntingtin fragment and concurrently accelerating fibrillization.

It has been hypothesized that polyQ repeats in huntingtin may function as polar zippers—that is, pleated sheets of β -strands held together by hydrogen bonds between main chain and side chain amides²⁴. Antibody-binding experiments in this study indicate that the polyQ repeat on HD53Q becomes buried as the protein assembles into spherical and annular structures, presumably owing to oligomerization between polyQ tracts in a solvent-excluded core. Consistent with the attenuation of spherical and annular structure formation observed by AFM, slot-blot analysis showed that Hsp70 and Hsp40 completely prevented the occlusion of polyQ epitopes that was observed when spherical and annular assemblies accumulated in the absence of chaperones. It is tempting to speculate that spherical and annular polyQ oligomers, or the process of their formation, may mediate the sequestration of transcription factors and/or other proteins that has been implicated in Huntington disease pathogenesis²⁵, and that chaperones may prevent this sequestration. It has recently been reported that Hsp70 and Hsp40 prevent an intramolecular conformational change in HD53Q (determined by fluorescence resonance energy transfer) that occurs <1 h after GST cleavage, and in doing so suppress heterotypic interactions between the mutant huntingtin fragment and transcription factors that contain a polyQ stretch²⁶. Although AFM analyses were not reported in this study, the experimental conditions used suggest that this chaperone-induced conformational change occurs before or concomitant with the formation of spherical structures. In the study presented here, sedimentation analyses of HD53Q aggregation reactions indicate that Hsp70 and Hsp40 maintain a substantial fraction of HD53Q in a SDS-soluble, monomeric conformation(s), similar to what has been reported when Hsp70 or Hsp40 are overexpressed in a fly model of polyQ disease¹⁸. The simplest interpretation of these results is that the cooperative activity of Hsp70 and Hsp40 prevents a structural transition in HD53Q that leads to potentially toxic off-pathway assemblies, and/or facilitates the folding and subsequent accumulation of a

fibril-competent misfolded HD53Q conformation that may be inert or protective. How might this occur? We speculate that Hsp70 and HD53Q monomers are in a rapid, dynamic equilibrium between the bound and free states. Binding of Hsp70 to HD53Q occurs in a Hsp40-dependent cycle, and each time HD53Q monomers are released they may undergo a kinetic partitioning between folding and native states, folding to a fibril-competent monomeric conformation and rebinding to Hsp70. Thus, under these conditions, a small percentage of HD53Q will always remain in a SDS-soluble monomeric state, whereas off-pathway spherical and annular structures will be diminished substantially. *In vitro* studies with the prion protein (PrP) have shown that GroEL, a homolog of human Hsp60, can catalyze the formation of aggregates with a high β -sheet content and protease resistance that is characteristic of the infectious form of the protein (PrP^{Sc}), suggesting that chaperones, typically thought of as preventing the aggregation of disease-causing proteins, may in some cases enhance aggregation²⁷. A recent study showed that under specific experimental conditions Hsp104 catalyzes the assembly of the Sup35 protein into fibrils²³. Furthermore, another study showed that in a yeast model of polyQ aggregation, loss of function mutations in the Hsp40 homologs *SIS1* and *YDJ1* suppress the aggregation of a mutant huntingtin fragment with an expanded polyQ repeat, whereas mutation of the Hsp70 homologs *SSA1* and *SSA2* inhibits the expansion of small, diffuse aggregate foci into an inclusion body²⁸.

Overexpression of Hsp70 suppresses neurodegeneration in mouse and *Drosophila melanogaster* models of polyQ disease^{18,29–31} and prevents dopaminergic neuron loss associated with α -synuclein toxicity in *D. melanogaster*³². Paradoxically, in these studies chaperone overexpression did not alter the number or morphology of inclusion bodies, calling into question the hypothesis that inclusion formation was a proximal event in disease pathogenesis. Consistent with the data presented in this study, the inclusions formed in the presence of chaperones in these models showed moderately enhanced solubility in SDS. Although spherical and annular structures may not be on-pathway for fibril formation by polyQ proteins, this does not imply that they may not be important in Huntington disease pathogenesis. Indeed, we propose that the ability of Hsp70 and Hsp40 to attenuate formation of these assemblies may account for their protective effects in animal models of neurodegenerative disease.

Note added in proof: Collins et al.³⁵ recently showed that the formation of amyloid fibrils by the yeast prion protein Sup35 can occur exclusively as the

result of monomer addition, and suggested that amyloid polymerization and oligomer assembly are competitive reactions, consistent with the model for polyQ shown in **Figure 7a**.

METHODS

Protein purification. GST HD20Q and HD53Q proteins were purified as described¹⁴. Fresh, unfrozen HD53Q and HD20Q proteins were used for all experiments. Hsp40 was expressed from the plasmid pQE9 in *E. coli* and purified as described³³. Hsp70 was expressed from the plasmid pMPM-A4 and purified from *E. coli* using the Morimoto lab purification protocol (<http://www.biochem.northwestern.edu/ibis/morimoto/protocols.html>). Chaperones were frozen in liquid nitrogen and stored at -80°C .

In vitro aggregation reactions. Before each experiment, HD20Q or HD53Q was centrifuged (20,000g) for 30 min at 4°C to remove pre-existing aggregates. HD20Q or HD53Q proteins were incubated at three different concentrations: 6, 20 or 60 μM in buffer A (50 mM Tris-HCl, pH 7, 150 mM NaCl, 1 mM DTT, 1 mM PMSF, 0.5 μM leupeptin, 0.5 μM pepstatinA). PreScission protease (4 units/100 μg fusion protein) (Amersham Biosciences) was added at time zero to initiate GST cleavage and aggregation of HD53Q. HD20Q remained soluble after GST cleavage. Hsp70 and Hsp40 proteins were added alone or in combination at an equimolar ratio to the fusion protein (6 or 20 μM) to the aggregation reactions at time zero or, alternatively, 1 h after aggregation was initiated with protease. Reactions containing Hsp70 were supplemented with 2 mM ATP, 50 mM KCl, 5 mM MgCl_2 and an ATP-regenerating system (50 $\mu\text{g ml}^{-1}$ creatine kinase and 8 mM creatine phosphate). Samples were incubated at 30°C in siliconized 1.5-ml eppendorf tubes, with shaking at 1,400 r.p.m. for up to 5 h.

Atomic force microscopy. AFM was used to analyze the morphology of aggregating HD53Q species over time in the presence or absence of chaperones. Aliquots of HD53Q or HD20Q protein were removed from the 6, 20 and 60 μM aggregation reactions, diluted into 50 mM Tris-HCl, pH 7, and immediately spotted on freshly cleaved mica. After two minutes the sample was washed with 200 μl distilled water, partially dried with compressed air, and completely dried at room temperature. The amount of protein spotted onto the mica is 1.3 μg for the 20 and 60 μM reactions and 0.65 μg for the 6 μM reactions. The samples were imaged in air with a digital multimode NanoscopeII scanning probe microscope operating in tapping mode (<http://www.veeco.com/>). The SPIP imaging program was used to carry out grain analysis, calculating the total number of fibrillar and nonfibrillar (spherical, annular and amorphous) assemblies in the 3 μm^2 AFM images (<http://www.imagemet.com/>). For each experimental condition, representative 3 μm^2 images obtained in three independent experiments were used to determine the average and s.d. for the density (particles/field) of fibrils and spherical, annular and amorphous structures at 1 and 5 h. A Student's *t*-test was used to determine whether the increase in fibril density (or decrease in the density of nonfibrillar assemblies) between 1 and 5 h was statistically significant ($P < 0.05$). Using SPIP, representative 3 μm^2 AFM images from at least three separate experiments were analyzed to determine the range and average length, width and height of spherical, annular and fibrillar structures observed under selected experimental conditions.

Slot-blot assay. At 0, 1 and 5 h after GST cleavage, equal amounts of protein (2 μg) were removed from 6, 20 and 60 μM aggregation reactions. Immediately, a dilution series was prepared in nondenaturing buffer A and 1 μg , 0.5 μg and 0.25 μg HD53Q or HD20Q protein was applied to a nitrocellulose membrane (0.2 μm pore size, Schleicher & Schuell) through a slot-blot manifold. Both soluble monomeric and aggregated forms of HD53Q are retained, in a nondenatured state, on this charged, high protein-binding membrane. The antibodies MW8, which recognizes the last eight amino acids of huntingtin exon 1 (AEEP LHRP) (1:1,000); 3B5H10, which was raised against the polyQ repeat of an expanded huntingtin exon 1 protein and binds in the polyQ region (1:10,000); MW7, which binds the two polyproline regions of the huntingtin exon 1 fusion protein³⁴ (1:350); and MW1, which binds an expanded polyQ repeat of the huntingtin exon 1 fusion protein³⁴ (1:350) were used to probe the nitrocellulose membranes. Huntingtin fragments were visualized with the ECL system (Amersham Biosciences). Representative blots are shown in **Figure 6**.

Centrifugal sedimentation assay. HD53Q (10 μg) protein was removed from an aggregation reaction at 0, 1 and 5 h after GST cleavage and centrifuged at

room temperature at 70,000 r.p.m. (230,000g) in a TLA 100.3 rotor for 20 min. SDS sample buffer was added to supernatant and pellet fractions, followed by heating at 95°C for 15 min. Supernatant and pellet fractions were resolved by SDS-PAGE and the MW8 antibody was used to visualize the huntingtin fragments. Representative blots are shown in **Figure 6f**. For quantification, blots were scanned and the pixel intensity of each band was measured using NIH image (<http://rsb.info.nih.gov/nih-image/Default.html>). The percentage of soluble material remaining at 1 and 5 h in the HD53Q samples with Hsp70 and Hsp40 was calculated by comparing the pixel intensity at 1 or 5 h to the pixel intensity at time zero in the soluble fraction. To calculate the percent decrease in insoluble material seen in the stacking gel at 1 and 5 h in the presence of Hsp70 and Hsp40, the pixel intensity of each time point with or without chaperones was compared. The results of three independent experiments were used to calculate the average and s.e.m.

Note: Supplementary information is available on the Nature Structural & Molecular Biology website.

ACKNOWLEDGMENTS

P.J.M. is supported by the US National Institute of Neurological Disorders and Stroke (R01NS47237), by a US National Institutes of Health (NIH) construction award (C06 RR 14571), by the Alzheimer's Disease Research Center at the University of Washington and by the Hereditary Disease Foundation under the auspices of the Cure Huntington's Disease Initiative. J.L.W. is funded in part by PHS NRSA T32 GM07270 from the US National Institute of General Medical Sciences. H.F., M.H.Z. and M.S. thank DURINT Program for support. AFM experiments were carried out in the Molecular Biomimetics Facilities at the University of Washington. We thank P. Patterson for the MW1-8 antibodies, S. Finkbeiner for the 3B5H10 antibody and M. Mayer and K. Terada for plasmids.

COMPETING INTERESTS STATEMENT

The authors declare that they have no competing financial interests.

Received 14 June; accepted 5 October 2004

Published online at <http://www.nature.com/nsmb/>

- Dobson, C.M. Protein folding and misfolding. *Nature* **426**, 884–890 (2003).
- Caughey, B. & Lansbury, P.T. Protofibrils, pores, fibrils, and neurodegeneration: separating the responsible protein aggregates from the innocent bystanders. *Annu. Rev. Neurosci.* **26**, 267–298 (2003).
- Walsh, D.M., Lomakin, A., Benedek, G.B., Condron, M.M. & Teplow, D.B. Amyloid β -protein fibrillogenesis. Detection of a protofibrillar intermediate. *J. Biol. Chem.* **272**, 22364–22372 (1997).
- Harper, J.D., Wong, S.S., Lieber, C.M. & Lansbury, P.T. Observation of metastable A β amyloid protofibrils by atomic force microscopy. *Chem. Biol.* **4**, 119–125 (1997).
- Lambert, M.P. *et al.* Diffusible, nonfibrillar ligands derived from A β 1–42 are potent central nervous system neurotoxins. *Proc. Natl. Acad. Sci. USA* **95**, 6448–6453 (1998).
- Conway, K.A., Harper, J.D. & Lansbury, P.T., Jr. Fibrils formed in vitro from α -synuclein and two mutant forms linked to Parkinson's disease are typical amyloid. *Biochemistry* **39**, 2552–2563 (2000).
- Conway, K.A. *et al.* Accelerated oligomerization by Parkinson's disease linked α -synuclein mutants. *Ann. NY Acad. Sci.* **920**, 42–45 (2000).
- Rochet, J.C., Conway, K.A. & Lansbury, P.T., Jr. Inhibition of fibrillization and accumulation of prefibrillar oligomers in mixtures of human and mouse α -synuclein. *Biochemistry* **39**, 10619–10626 (2000).
- Ding, T.T., Lee, S.J., Rochet, J.C. & Lansbury, P.T. Jr. Annular α -synuclein protofibrils are produced when spherical protofibrils are incubated in solution or bound to brain-derived membranes. *Biochemistry* **41**, 10209–10217 (2002).
- The Huntington's Disease Collaborative Research Group. A novel gene containing a trinucleotide repeat that is expanded and unstable on Huntington's disease chromosomes. *Cell* **72**, 971–983 (1993).
- Scherzinger, E. *et al.* Huntingtin-encoded polyglutamine expansions form amyloid-like protein aggregates *in vitro* and *in vivo*. *Cell* **90**, 549–558 (1997).
- Hartl, F.U. & Hayer-Hartl, M. Molecular chaperones in the cytosol: from nascent chain to folded protein. *Science* **295**, 1852–1858 (2002).
- Muchowski, P.J. Protein misfolding, amyloid formation, and neurodegeneration: a critical role for molecular chaperones? *Neuron* **35**, 9–12 (2002).
- Muchowski, P.J. *et al.* Hsp70 and hsp40 chaperones can inhibit self-assembly of polyglutamine proteins into amyloid-like fibrils. *Proc. Natl. Acad. Sci. USA* **97**, 7841–7846 (2000).
- Scherzinger, E. *et al.* Self-assembly of polyglutamine-containing huntingtin fragments into amyloid-like fibrils: implications for Huntington's disease pathology. *Proc. Natl. Acad. Sci. USA* **96**, 4604–4609 (1999).
- Fewell, S.W., Day, B.W. & Brodsky, J.L. Identification of an inhibitor of hsc70-mediated protein translocation and ATP hydrolysis. *J. Biol. Chem.* **276**, 910–914 (2001).
- Kayed, R. *et al.* Common structure of soluble amyloid oligomers implies common mechanism of pathogenesis. *Science* **300**, 486–489 (2003).

18. Chan, H.Y., Warrick, J.M., Gray-Board, G.L., Paulson, H.L. & Bonini, N.M. Mechanisms of chaperone suppression of polyglutamine disease: selectivity, synergy and modulation of protein solubility in *Drosophila*. *Hum. Mol. Genet.* **9**, 2811–2820 (2000).
19. Giasson, B.I. *et al.* Initiation and synergistic fibrillization of τ and α -synuclein. *Science* **300**, 636–640 (2003).
20. Poirier, M.A. *et al.* Huntingtin spheroids and protofibrils as precursors in polyglutamine fibrillization. *J. Biol. Chem.* **277**, 41032–41037 (2002).
21. Tanaka, M. *et al.* Expansion of polyglutamine induces the formation of quasiaggregate in the early stage of protein fibrillization. *J. Biol. Chem.* **278**, 34717–34724 (2003).
22. Chen, S., Ferrone, F.A. & Wetzel, R. Huntington's disease age-of-onset linked to polyglutamine aggregation nucleation. *Proc. Natl. Acad. Sci. USA* **99**, 11884–11889 (2002).
23. Shorter, J. & Lindquist, S. Hsp104 catalyzes formation and elimination of selfreplicating Sup35 prion conformers. *Science* **304**, 1793–1797 (2004).
24. Perutz, M.F., Johnson, T., Suzuki, M. & Finch, J.T. Glutamine repeats as polar zippers: their possible role in inherited neurodegenerative diseases. *Proc. Natl. Acad. Sci. USA* **91**, 5355–5358 (1994).
25. Sugars, K.L. & Rubinsztein, D.C. Transcriptional abnormalities in Huntington disease. *Trends. Genet.* **19**, 233–238 (2003).
26. Schaffar, G. *et al.* Cellular toxicity of polyglutamine expansion proteins: mechanism of transcription factor deactivation. *Mol. Cell* **15**, 95–105 (2004).
27. Stockel, J. & Hartl, F.U. Chaperonin-mediated *de novo* generation of prion protein aggregates. *J. Mol. Biol.* **313**, 861–872 (2001).
28. Meriin, A.B. *et al.* Huntington toxicity in yeast model depends on polyglutamine aggregation mediated by a prion-like protein Rnq1. *J. Cell Biol.* **157**, 997–1004 (2002).
29. Warrick, J.M. *et al.* Suppression of polyglutamine-mediated neurodegeneration in *Drosophila* by the molecular chaperone HSP70. *Nat. Genet.* **23**, 425–428 (1999).
30. Kazemi-Esfarjani, P. & Benzer, S. Genetic suppression of polyglutamine toxicity in *Drosophila*. *Science* **287**, 1837–1840 (2000).
31. Cummings, C.J. *et al.* Over-expression of inducible HSP70 chaperone suppresses neuropathology and improves motor function in SCA1 mice. *Hum. Mol. Genet.* **10**, 1511–1518 (2001).
32. Auluck, P.K., Chan, H.Y., Trojanowski, J.Q., Lee, V.M. & Bonini, N.M. Chaperone suppression of α -synuclein toxicity in a *Drosophila* model for Parkinson's disease. *Science* **295**, 865–868 (2002).
33. Minami, Y., Hohfeld, J., Ohtsuka, K. & Hartl, F.U. Regulation of the heat-shock protein 70 reaction cycle by the mammalian DnaJ homolog, Hsp40. *J. Biol. Chem.* **271**, 19617–19624 (1996).
34. Ko, J., Ou, S. & Patterson, P.H. New anti-huntingtin monoclonal antibodies: implications for huntingtin conformation and its binding proteins. *Brain Res. Bull.* **56**, 319–329 (2001).
35. Collins, S.R., Dougllass, A., Vale, R.D. & Weissman, J.S. Mechanism of prion propagation: amyloid growth occurs by monomer addition. *PLoS Biol.* **2**, E321 (2004).